Supplementary Information (SI) for Nanoscale.
This journal is © The Royal Society of Chemistry 2024

Supplementary Information

Contents:

Section S1: Materials and methods

S1.1 Materials

MoS_2 bulk powder (Asbury Graphite Mills, Inc.), n-hexane and n-Butyllithium (Carbanio), and distilled water (Millipore water purification system of conductivity 18.2 MΩ) were utilized for the study. All reagents were used as such without any further purification. PVDF supporting membranes (pore size = 0.22 µm) were purchased from Merck.

S1.2 Physical characterization and sample preparation

Surface morphology and elemental analysis of the MoS_2 nanosheets were done using FE-SEM, JSM7600F with Oxford energy dispersive X-ray spectroscopy (EDX) attachment. The as-prepared membranes were analyzed in SEM in surface and cross-sectional modes. For cross-sectional analysis, the membrane was torn to expose the layers. The crystalline structure of prepared MoS_2 nanosheets was determined by X-ray diffraction studies using an automated multipurpose X-ray diffractometer by Rigaku SmartLab at 1.54 Å Cu Kα. XRD was done on a whole membrane or its smaller part. Raman measurements were performed with an ALPHA300 R Confocal Raman Microscope (WITec) using 532 nm laser (0.8 mW power) for excitation at room temperature. XPS spectra were acquired with an ESCALAB 250 XI (Thermo Fisher Scientific, Source: Al Kα 1486.6 eV, 650 µm spot size, Pass energy: 40 eV with hemispherical analyzer) system with an analysis chamber maintained in ultrahigh vacuum (UHV ~ 5×10^{-10} mbar) conditions. The functional groups in the membranes were analyzed by using a Fourier transform infrared (FTIR) spectrometer. Samples for ultraviolet-visible spectroscopy and zeta potential measurement were prepared by diluting the master solution with DI water in a ratio of 1:10.

Section S2: Figures

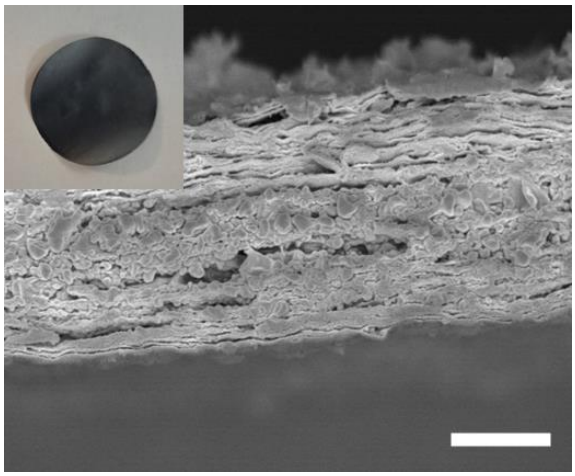

Fig. S1. Cross-sectional SEM image of a 2H MoS_2 membrane. Scale bar 500 nm. Inset: camera image of a freestanding membrane. Although the cleaving of the membrane is not proper, the laminate structure is still observed clearly.

S2.1 van der Waals gap in MoS_2 phases

In the context of 2D materials, van der Waals distance and van der Waals gap are essentially different terms. The interlayer space, also called d spacing, is the space between two consecutive MoS_2 layers. This is calculated from the XRD analysis using the Bragg's law, $2\,d\sin\theta = n\lambda$. This d is called the van der Waals distance (d_{vdW}). However, not all of this interlayer space is available for transport, as some space is also occupied by the electron cloud. The free space that is available for the transport of a species is called van der Waals gap (h_{vdW}). This is calculated by subtracting the thickness of one layer of MoS_2, i.e. 6.5 Å., from the d spacing.

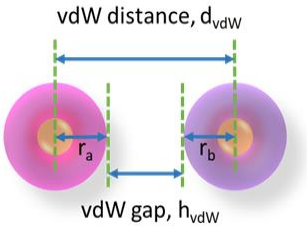

$$h_{vdW} = d_{vdW} - (r_a + r_b)$$

Fig. S2. Schematic representation of van der Waals gap.

For 2H phase, from XRD data, we have d_{vdW} (2H MoS_2) = 6.5 Å.

∴ h_{vdW} (2H MoS_2) = 6.5 Å - 6.5 Å = 0.

The van der Waals gap in 2H MoS_2 is negligible.

For 2H MoS_2, d_{vdW} = 6.5 Å. Due to its compact structure, we take 6.5 Å as the upper bound to estimate the h_{vdW} in 1T' MoS_2 as follows:

$$h_{vdW} = d_{vdW} - (r_a + r_b)$$

From XRD data, we calculated d_{vdW} (1T' MoS_2) = 12.5 Å,

And let $r_a + r_b$ = 6.5 Å,

∴ h_{vdW} (1T' MoS_2) = 12.5 Å - 6.5 Å = 6 Å

Hence, h_{vdW} for 1T' MoS_2 is 6 Å.

S2.2 XPS Characterization

X-ray photoelectron spectroscopy (XPS) was used for phase confirmation of the synthesized 1T' MoS_2 and 2H MoS_2. The peaks of 1T' phase are downshifted by ≈0.5 eV compared to the 2H phase. In the Li-intercalated 1T' phase, the Mo 3d core level peaks chemically shift such that its binding energies are lower than that of 2H phase. The decrease in binding energy is due to the chemical reduction of Mo from the +4 to the +3-oxidation state.

S vacancies: Ideally, in a defect free MoS_2, the ratio S:Mo is 2:1. In our case, for 1T' phase membrane, S:Mo = 1.32:1, whereas for 2H phase membrane, S: Mo = 1.35:1. This is summarized in the following table:

Case	**Ideal**	**1T'**	**2H**
S:Mo Ratio	2:1	1.32:1	1.35:1

From XPS, we can infer that S vacancies are indeed present in both our phases. In fact, 1T' phase has higher number of S vacancies than the 2H phase.

Please note that the XPS data for both the phases was taken after a week of the sample preparation, as the samples were in transit to another institute for analysis. This might have slightly affected the composition of the 1T' MoS_2 membrane.

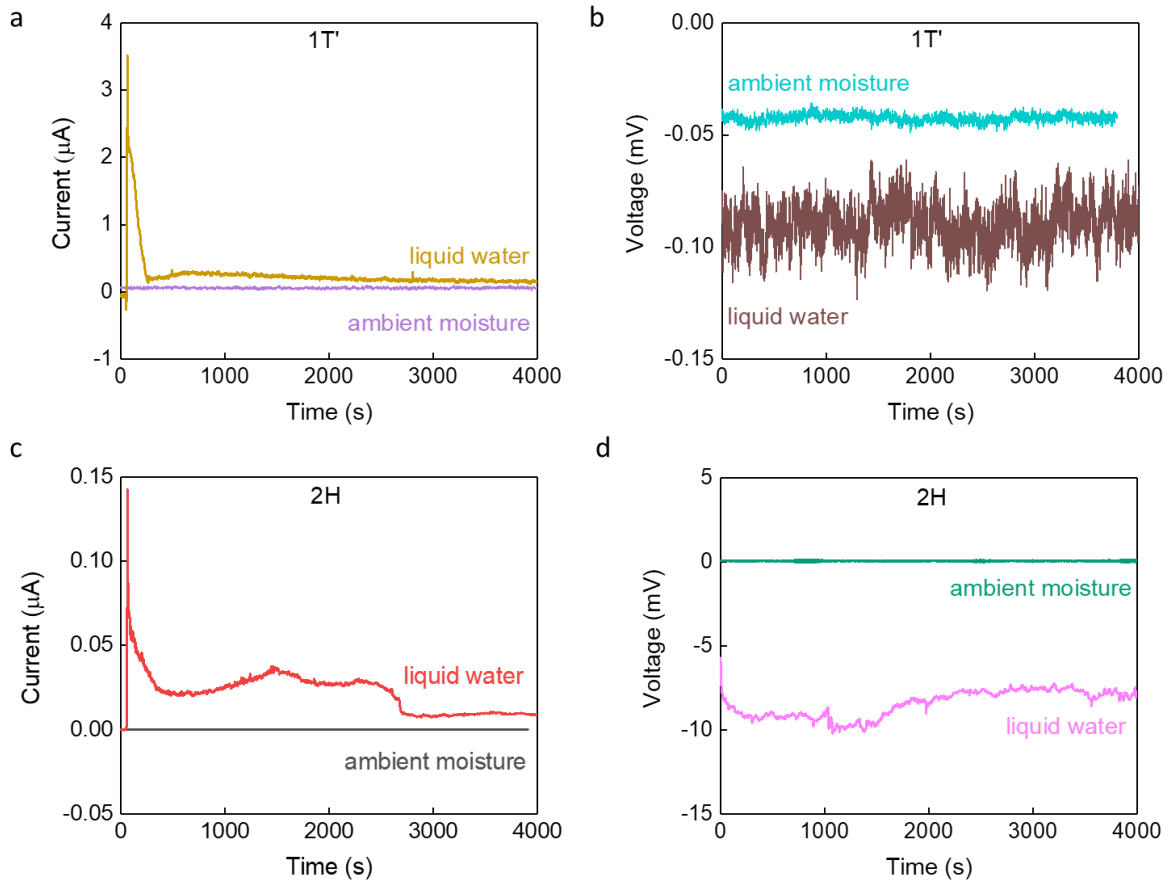

Fig. S3. Variation of current and potential with time. a. and b. 1T' devices. **c. and d.** 2H devices. When the water is added to the beaker, both devices have an instantaneous increase in the current level, which can be seen from the spike just after t = 0.

S2.3 Additional experiments

To prove conclusively that the streaming current is in fact driven by evaporation, we further demonstrate that there is a strong dependency on the environmental conditions such as humidity and air flow, by performing additional experiments with a 1T' device as follows:

a) Firstly, during the measurement, the EEG was sealed properly using parafilm, and it was observed that the current level gradually dropped. When the device was unsealed again, the current regained its value. This was repeated a few times for different time intervals.
b) Secondly, air flow was turned on above the EEG, and it was observed that the current level increased. This is because the water evaporates faster in the wind. Such change could be completely repeated.

These experiments confirm that evaporation is the origin of the induced current.

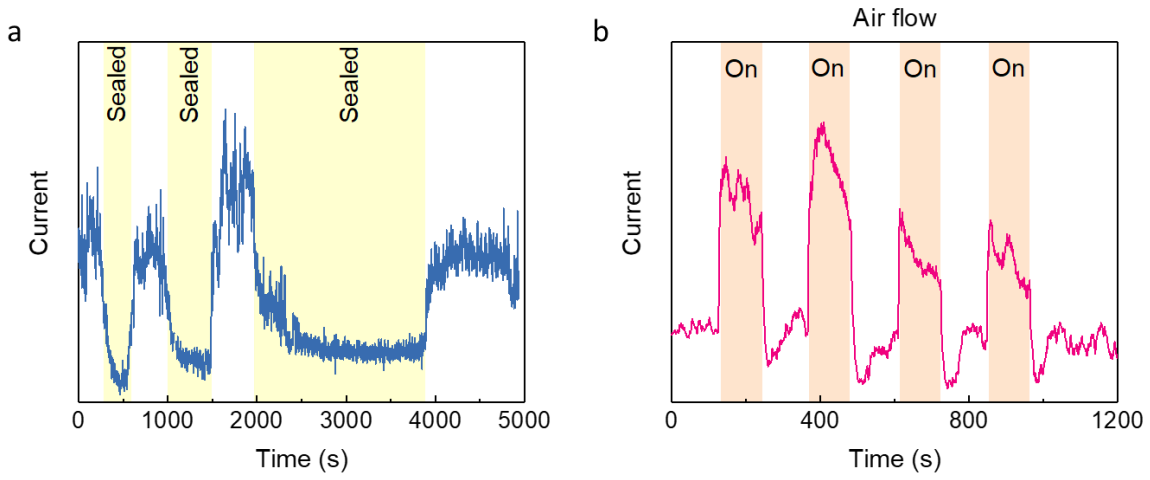

Fig. S4. Experiments to determine the effect of change in evaporation rate. a. The EEG was sealed inside the beaker, and then unsealed. The dropping of current by 90% inside the sealed device is due to slower evaporation. **b.** The air flow was turned on and off above the EEG. The current increased by 12 times with the air flow due to faster evaporation.

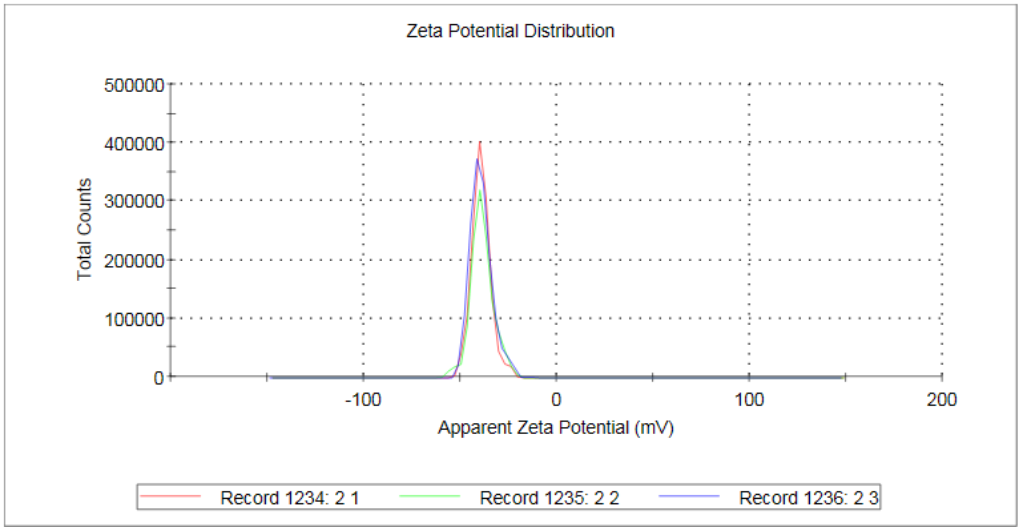

Fig. S5. Zeta Potential of 1T' MoS_2 dispersion. Zeta Potential measurements of the provided a mean value of -38.8 mV. The different curves are from three different measurements.

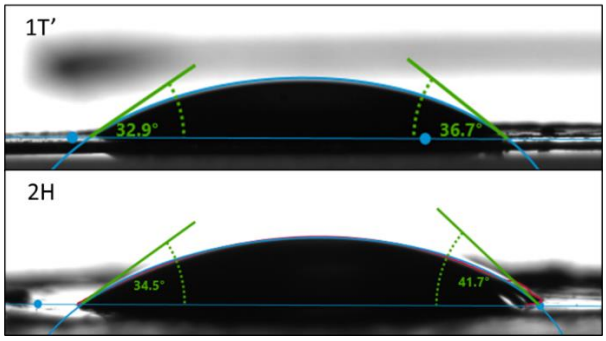

Fig. S6. Contact angle measurement of 1T' and 2H MoS_2 membranes. The contact angle for 1T' phase ≈34° and for 2H phase ≈37°.

S2.4 FTIR Analysis

1T' and 2H phases membranes were analyzed using FTIR spectrometer. The 463 cm^{-1} peak in 1T' phase corresponds to the Mo-S bond. The 1T' phase shows a water bonding peak[1] at 1600 cm^{-1} which indicates the presence of water trapped between its interlayers, as also indicated by the XRD data. This peak is absent in the 2H phase, whereas it shows other peaks, such as S-S bond[2] at 808 cm^{-1}, and -OH bond[3] at ~3332 cm^{-1}.

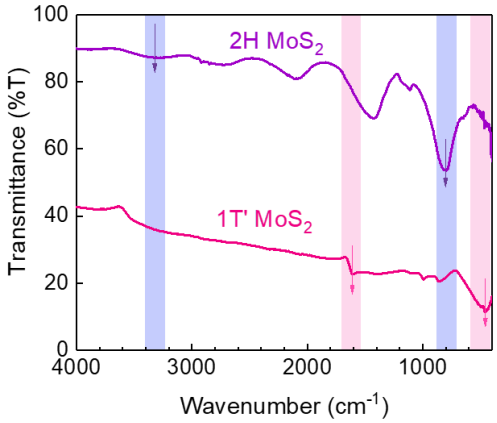

Fig. S7. FTIR analyses of two MoS_2 phases

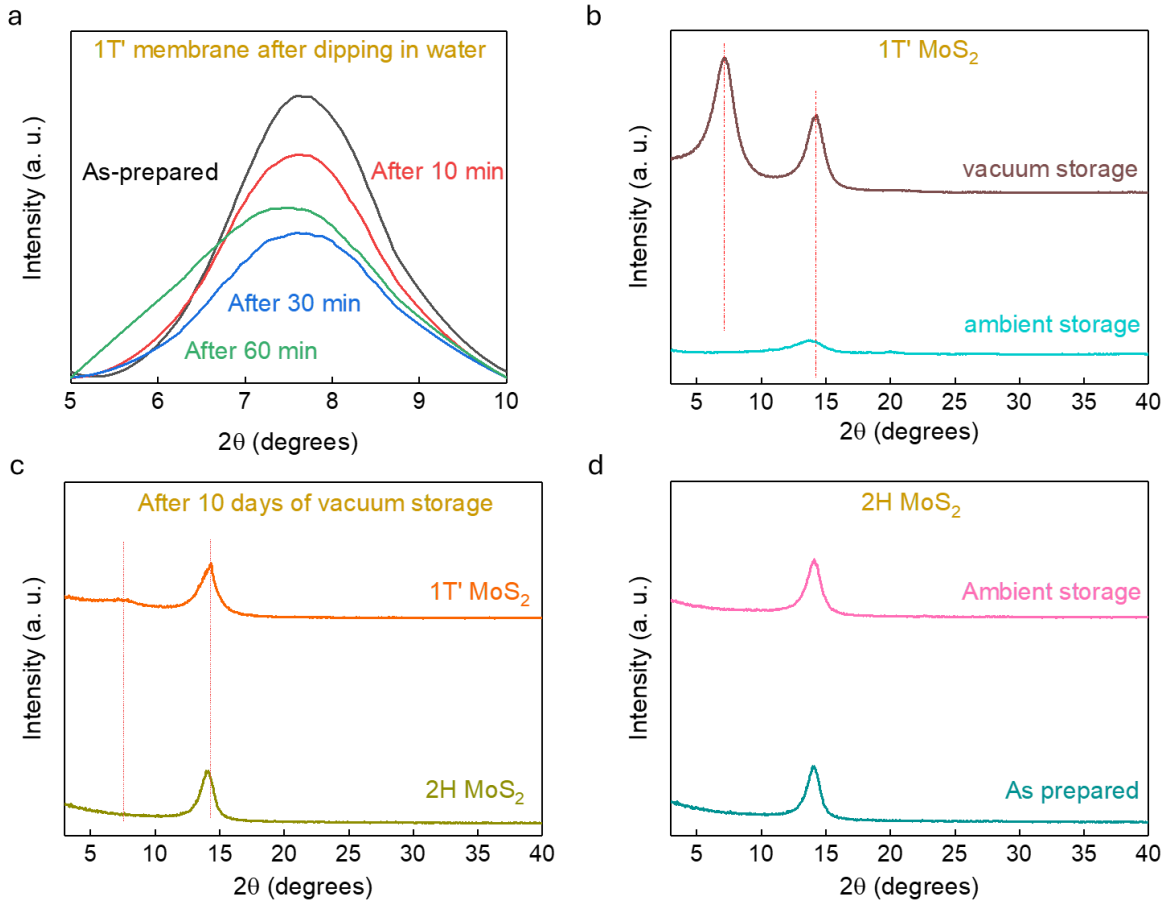

Fig. S8. X-ray diffraction data for analyzing the stability of 1T' MoS_2 and 2H MoS_2. a. 1T' phase in contact with water. **b.** Effect of storage condition on the metastable 1T' phase- the 1T' phase is lost if the membrane is stored in the ambient environment. **c.** Decay of 1T' phase over time, even after storage in a vacuum. **d.** Effect of storage condition on the 2H phase- no change is observed over a long time.

Section S3: Theoretical estimation of Streaming Current and Potential

The streaming current and potential due to external pressure difference ΔP are given by:

$$I_S = \frac{A\,\varepsilon_0\,\varepsilon_r\,\Delta P\,\xi}{\eta L} \quad \text{....(1)}$$

$$V_S = \frac{\varepsilon_0\,\varepsilon_r\,\Delta P\,\xi}{\eta\sigma} \text{....(2)}$$

where L is channel length, A is the pore cross-sectional area and ζ is the internal surface zeta potential, ε_0 is the vacuum permittivity, ε_r dielectric constant of the liquid, σ conductivity of the fluid-saturated porous medium, and η liquid viscosity, respectively.

The channel length for the calculations is taken as L = distance between electrodes E1 and E2 = 5 mm, and the thickness of the membranes, t = 1 μm.

- *For a 1T' MoS_2 membrane:*

ΔP is the capillary pressure given by $\Delta P = 4\gamma cos\theta/d$, where θ is water contact angle, γ is the surface tension of water, and d is the diameter of the channel (capillary/ pore).

Considering γ = 0.072 N.m^{-1}, θ = 34˚, and d = 6 Å (the h_{vdW} of 1T' phase),

$\Delta P = 4\gamma cos\theta/d$ = 3.98 kbar = ~4 kbar

Pore cross-sectional area was calculated as $A = \pi d^2/4 = 2.82 \times 10^{-19}$. The width of 1T' membrane was 11 mm. Now, $\varepsilon_0 = 8.854 \times 10^{-12}$ F m^{-1}, $\varepsilon_r = 3$[4,5], η = 0.89 mPa.s.

Total no. of channels, n = $\frac{t \times w}{A} = 3.9 \times 10^{10}$.

The conductivity σ of 1T' phase was estimated from the slope of the I-V graph as 9.09×10^2 S m^{-1} = ~10^3 S m^{-1}.

Eqn (1) would give the current for one channel, so it must be multiplied with the total number of channels responsible for water intake. This could be calculated as follows:

Substituting the above values in eqn (1) × n,

$I_S = 1.0 \times 10^{-6}$ A.

The factor n has already been considered while calculating σ, so from eqn (2),

$V_S = 5.1 \times 10^{-4}$ V.

Power density = $\frac{I_S \times V_S}{A}$ = 46.7 mW m^{-2}

- *For a 2H MoS_2 membrane:*

The σ was estimated from the slope of the I-V graph as 1.8×10^{-4} S m^{-1}. Due to lack of well-defined channels,

(i) A is the area between the two electrodes E1 and E2. $A = L \times$ w (w = width of the membrane) = 5 mm × 7 mm.

(ii) ΔP is the saturated vapor pressure = 23 mbar.

Substituting these values in eqn (1) and eqn (2),

$I_S = 1.6 \times 10^{-8}$ A, and

$V_S = 12.9$ mV.

Power density = $\frac{I_S \times V_S}{A}$ = 5.8×10^{-3} mW m^{-2} = 5.8 μW.m^{-2}

- *For a purely surface contribution in 1T' phase:*

The σ can be estimated from slope of the I-V graph as 0.18 S m^{-1}.

(i) A is the area between the two electrodes E1 and E2. $A = L \times$ w (w = width of the membrane) = 5 mm × 11 mm.

(ii) ΔP is the saturated vapor pressure = 23 mbar.

Substituting these values in eqn (1) and eqn (2),

I_S(surface, 1T') = 3.0×10^{-8} A, and

V_S (surface, 1T') = 1.5×10^{-5} V.

Power density (surface, 1T') = $\frac{I_S \times V_S}{A}$ = 7.8 nW m^{-2}

Since the surface contribution is three orders of magnitude less than the channel contribution, it would not make a significant difference to the overall values of current and power density.

Supplementary Table 1. Comparison between 1T' and 2H phases of MoS_2.

Characterization/Properties	1T'	2H
Phase	metallic	semiconducting
Thermal stability	metastable	stable
Channel structure	well-defined channels	no channels
Interlayer spacing	12.5 Å	6.5 Å
van der Waals gap	6 Å	-
Contact angle	≈34° (hydrophilic)	≈37° (hydrophilic)
Zeta Potential	-38.8 mV	-33 mV
Power density in contact with water	2.0 $mW.m^{-2}$	2.4 $\mu W.m^{-2}$
Power density in ambient	0.1 $mW.m^{-2}$	0.2 $pW.m^{-2}$
Path of water transport	Surface water diffusion (across the flakes) and along the channels	Surface water diffusion (across the flakes) only

Supplementary References

1 K. Zhou, S. Jiang, C. Bao, L. Song, B. Wang, G. Tang, Y. Hu and Z. Gui, *RSC Adv.*, 2012, **2**, 11695–11703.

2 T. Nagarajan, M. Khalid, N. Sridewi, P. Jagadish, S. Shahabuddin, K. Muthoosamy and R. Walvekar, *Sci. Rep.*, 2022, **12**, 14108.

3 G. A. M. Ali, M. R. Thalji, W. C. Soh, H. Algarni and K. F. Chong, *J. Solid State Electrochem.*, 2020, **24**, 25–34.

4 M. Belete, S. Kataria, U. Koch, M. Kruth, C. Engelhard, J. Mayer, O. Engström and M. C. Lemme, *ACS Appl. Nano Mater.*, 2018, **1**, 6197–6204.

5 E. J. G. Santos and E. Kaxiras, *ACS Nano*, 2013, **7**, 10741–10746.